U-006-105.7

167

STUDY AND EVALUATION OF K-65 SILOS FOR THE FEED MATERIALS PRODUCTION FACILITY AT FERNALD, OHIO

1-1-90

BNI/DOE
DE-ACO5-81OR20722
50
REPORT

[redacted]

Bechtel National, Inc.

STUDY AND EVALUATION OF K-65 SILOS FOR THE FEED MATERIALS PRODUCTION FACILITY AT FERNALD, OHIO

DOE/OR/DE-AC05-81OR20722

4.29 1590.1

167

Study and Evaluation of K-65 Silos for the Feed Materials Production Facility at Fernald, Ohio

January 1990

Prepared for
United States Department of Energy
Oak Ridge Operations Office
Under Contract No. DE-AC05-81OR20722

By

Bechtel National, Inc.
Oak Ridge, Tennessee

Bechtel Job No. 14501

2

CONTENTS

LIST OF TABLES iv

LIST OF FIGURES v

1.0 INTRODUCTION 1
1.1 Background 1
1.2 Objectives 3

2.0 APPROACH 5

3.0 SUMMARY 7

3.1 Conclusions 7
3.2 Recommendations 10

4.0 DISCUSSION OF RISKS 12

5.0 FIELD INVESTIGATIONS 14

6.0 MATERIAL TESTING 16
6.1 Concrete Strength Testing 16
6.2 Petrographic Analysis 17
6.3 Results of Material Testing 18

7.0 STRUCTURAL ANALYSIS 19
7.1 Finite-Element Models 19
7.2 Loads and Load Combinations 22
7.3 Discussion of Results 23

8.0 REFERENCES 44

APPENDIXES - Bound Separately

A Conclusions Excerpted from Camargo Reports

B Documentation Provided to Bechtel National, Inc., by Westinghouse Materials Company of Ohio

C Letter, Donald E. Graham to R. B. Barber, Bechtel National, Inc. "Job # 14501, FUSRAP Project Fernald K-65 Silos - Silo #4 Evaluation of Concrete," CCN 65196, November 27, 1989.

D Instruction Guide Work Plan for the Silo 4 Sampling at the Feed Materials Production Center Fernald, Ohio, 191-IG-010, Revision 1.

E Photographic Record of Field Activities

F Photographs of Selected Core Samples

G Letter, George Patrick, Geotek Engineering Company to R. B. Barber, Bechtel National, Inc. "Summary of Unconfined Compressive Strength and Splitting Tensile Strength Test Data," CCN 64803, November 8, 1989.

H Letter, Scott F. Wolter, Twin City Testing Corp. to David Chen, Bechtel National, Inc. "Report of Hardened Concrete Testing," CCN 64865, November 16, 1989.

I Silo Model Data and Analysis Results

(67

LIST OF TABLES

Table		Page
4-1	Comparative Risk of Uncontrolled Release of Radon. . . .	13
7-1	Load Combinations.	29
7-2	Comparison of Selected Stresses Obtained in Previous and Present Studies	30
7-3	Membrane Stresses in the Dome Obtained Using Model 1 . .	31
7-4	Membrane Stresses in the Dome Obtained Using Model 2 . .	32
7-5	Membrane Stresses in the Dome Obtained Using Model 3 . .	33
7-6	Stresses in the Silo Wall Using Model 3.	34
7-7	Model 3 Maximum Stresses and Allowables.	35
7-8	Dome Compressive Stresses Under Dead Plus Live Loads and Allowables Using Model 3.	36
7-9	Stresses in the Silo Wall for Selected Load Combinations	37

5

LIST OF FIGURES

Figure		Page
1-1	K-65 Silo Sections	4
7-1	Finite-Element Model of Silo	20
7-2	Deformed Shape - Dead Load	38
7-3	Deformed Shape - Live Load	39
7-4	Deformed Shape - Contents Pressure	40
7-5	Deformed Shape - Embankment Pressure	41
7-6	Hoop Forces in Dome - Live Load Only	42
7-7	Hoop Forces in Wall - Dead Load Only	43

1.0 INTRODUCTION

1.1 Background

As part of the U.S. Department of Energy (DOE) Feed Material Production Center (FMPC) Five-Year Environmental, Safety and Health Improvement Plan, studies have been conducted of four concrete waste storage silos . The silos are located in the K-65 and Metal Storage Area on the west side of the Fernald site. They were constructed during 1951 and 1952 for dewatering and storing radioactive waste effluent from the plant processing lines. Concrete placement for all four silos occurred during the fall and winter months. Silos 1 and 2 contain high-grade pitchblende ore (K-65) residue; Silo 3 contains metal oxide. Silo 4 has never been used.

By 1963, the silos were showing signs of exterior surface deterioration and a program of repairs was begun. In 1964, repairs were made to the shot-crete coat, and an earthen embankment was constructed around Silos 1 and 2 to counterbalance the load from the silo contents. The embankment also protects the walls from further weathering and acts as a deterrent to radon emission from the silos. Vents in the silos were sealed in 1979, and the embankments were enlarged in 1983 to reduce erosion. (For more detailed information on the history of the silos refer to the Camargo reports, Refs. 1-1, 1-2.)

In 1985, Camargo Associates, Limited (Camargo) performed non-destructive tests on the tanks to determine the condition of the concrete. Finite-element analysis was performed to determine structural stability and identify potential structural problem areas that may require remedial action. The conclusions reached as a result of those tests and analyses by Camargo (Ref. 1-1) have been excerpted and presented in Appendix A and are summarized as follows:

1) The analysis showed the center portions of Silos 1 and 2 to be structurally defective and have no life expectancy. This part of each dome was the most critical area under tornado loads.

2) It was recommended that the contents of Silos 1 and 2 be removed and disposed of properly.

3) Pending removal of the silo contents, it was recommended that a temporary self-supporting cover be installed over the portions of the domes identified in the analysis as defective areas.

As a continuation of their original study, Camargo also tested Silo 3, which contains metal oxide, and Silo 4, which is empty (Ref. 1-2). The results of those tests and analyses are summarized as follows:

1) The domes for both silos were determined to be in good condition, but there were a few areas of deterioration. Silo 4 was slightly more deteriorated than Silo 3. Most of the deterioration was in the posttensioning wires. Under either tornado or earthquake loading, the domes were the critical elements and would experience cracking, but the silos were expected to remain standing.

2) The walls of both silos were in good condition, but like the domes, had shown some deterioration, mostly in the post-tensioning wires.

3) Some cracking and deterioration, caused by freezing and thawing, could be seen in the base slabs of the silos.

Several corrective measures were taken by DOE as a result of the Camargo analysis, as shown in Figure 1-1. In January 1986, protective covers for the center portions of the domes of Silos 1 and 2 were constructed and put in place. The installation of waterproof protective membranes over the tops of the silos began in April 1986. In late 1987, a foam coating was applied to the domes to further reduce weathering, temperature changes inside the silos, and radon gas emissions. A radon treatment system was developed to remove radon from the silos before work was performed.

During July and August 1989 an investigative team ("Tiger Team") consisting of DOE and DOE contractor personnel conducted an investigation of the FMPC. One of the findings of that team was the identification of the potential for structural failure of the K-65 silos. As a result of that finding, Bechtel National, Inc. (BNI), the Formerly Utilized Sites Remedial Action Program (FUSRAP) program management contractor, was tasked to perform additional testing and analyses of the silos.

1.2 Objectives

The purpose of the testing and analysis described in this report was to:

- Determine the present state of structural integrity of the K-65 silos and perform an independent verification of the previous structural analyses performed by Carmargo.

- Verify the in-situ compressive strength of the tank concrete.

- Provide a qualitative assessment of the risk of structural failure of the tanks.

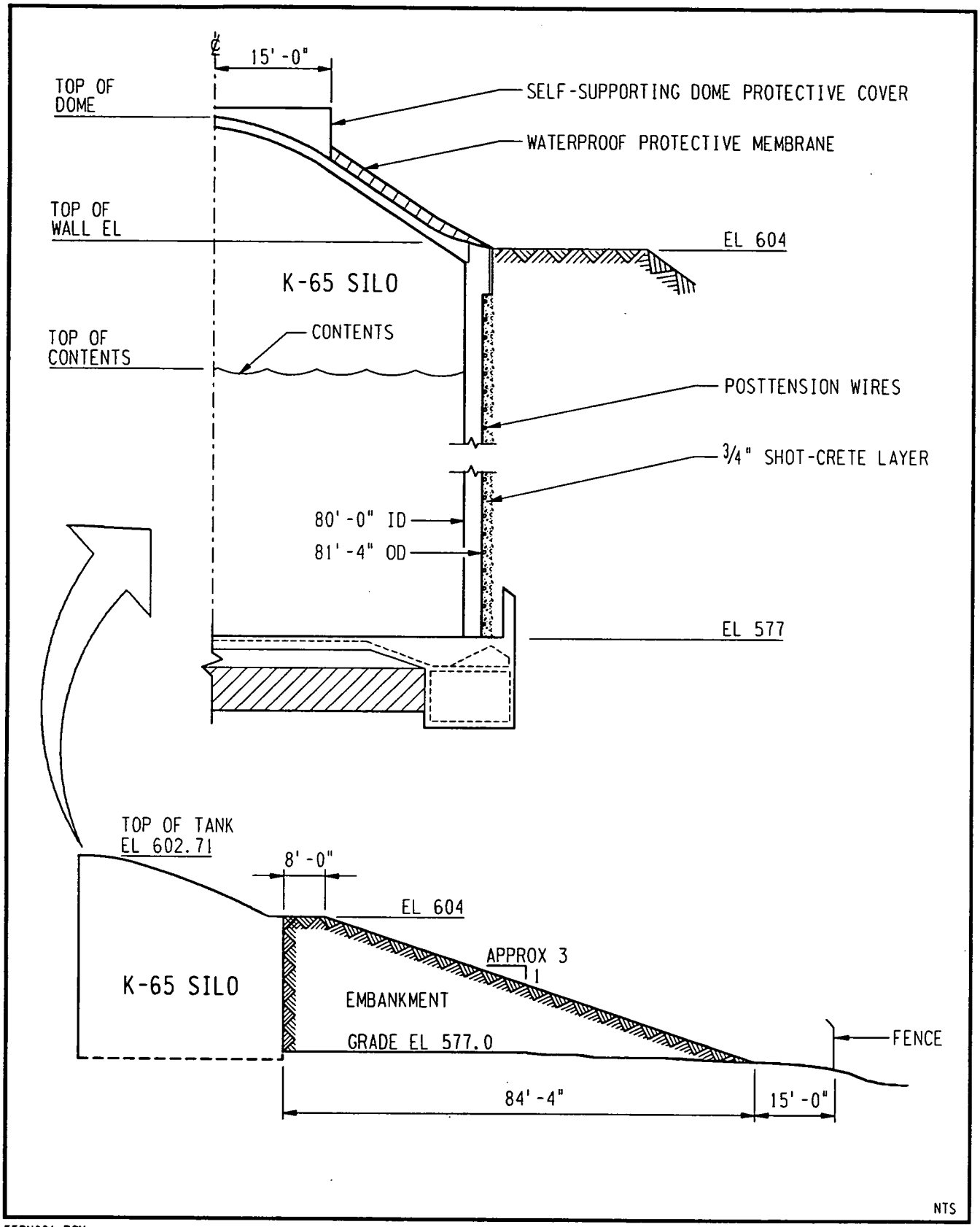

FERN001.DGN

FIGURE 1-1
K-65 SILO SECTIONS

2.0 APPROACH

Westinghouse Materials Company of Ohio (WMCO), the FMPC operation and maintenance contractor, supplied BNI with copies of the available documentation on original design, nondestructive testing, and remedial repair generated since completion of the construction of the silos in 1952 (Appendix B). These data were used as a baseline for comparison with the BNI testing and analysis program. The BNI study consisted of field investigations (Phase 1), materials testing (Phase 2), and structural modeling and analysis (Phase 3).

Phase 1 of the BNI investigation was a visual inspection of Silos 3 and 4. The structural components of Silos 1 and 2 could not be inspected because of the earthen embankment, steel cap, and foam cover.

Phase 2 of the BNI investigation began by obtaining concrete core samples from Silo 4. Core samples of the dome, wall, and floor were obtained for compressive strength testing and petrographic analysis. An additional core sample was obtained from the silo wall for tensile strength testing. A sample of the shot-crete covering over the reinforcing wire windings was obtained for petrographic analysis. The results of materials testing are discussed in Section 6.

The dome and floor samples were full-penetration cores. The wall samples did not fully penetrate the wall in order to preclude cutting the horizontal posttensioned reinforcing wire windings. The wall and floor samples were obtained from the interior of the silo.

Petrographic analysis was performed to determine reactivity of the aggregate, air content, and general condition of the concrete and shot-crete used in silo construction.

Phase 3 of the investigation consisted of structural modeling and analysis. Structural drawings and previous analytical reports were used to develop three-dimensional finite-element models of Silo 1 as representative of both K-65 silos. Three models were developed:

Model 1 - Silo 1 using the same material properties and configuration as used by Camargo in their 1986 report.

Model 2 - Same as model 1, but with addition of the cap structure to the model. The cap structure was added after the 1986 analysis.

Model 3 - Same as model 2, but with material properties revised based on the Phase 2 material testing reports.

Two load cases[1] were not analyzed because they do not represent existing or expected future loading conditions. A third load case, which includes seismic loading, was not analyzed because the Camargo analysis indicated that it was not a critical load case and was therefore not included in BNI's scope of work.

The analysis results of Model 1 were compared to the Camargo analysis as a check on the new model and as a verification of the Camargo results. The results of Model 2 evaluate the effect of adding the self-supporting steel cover over the center of the dome. The results of Model 3 evaluate the stability of the K-65 silos based on their current configuration and the current material properties obtained through testing of the concrete samples from Silo 4.

---

[1] **Camargo report load case 3 (Silo without the earthen embankment) and load case 6 (silo with 3 ft. soil cover over the dome).**

3.0 SUMMARY

3.1 Conclusions

Material testing of the concrete cores obtained from Silo 4 consisted of both strength tests and petrographic analyses. The strength tests showed that the concrete in the dome has retained less than 30 percent of their original 28-day compressive strength; the concrete in the walls have retained less than 40 percent. The petrographic analyses determined that the concrete has degraded to the point where all core samples are badly fractured, although we cannot assume uniformity throughout the structure, or that the same concrete conditions exist in Silos 1 and 2 (where the K-65 residues are stored). It is reasonable to assume that most, if not all, of the silo concrete is in a similar degraded condition (see Appendix C). All four silos were built during the fall and winter months and have been exposed to the same weather conditions for over 34 years.

The BNI analytical model is different from that used in the Camargo study. However, the results of the current model and analysis generally agree with those presented in the Camargo report. Although some discrepancies were discovered (as discussed in Section 7.3), they were not sufficient to invalidate the conclusions of either study.

The allowable stress approach was used to evaluate the silos. The allowable stresses were computed based on the reinforcement shown in the design drawings for Silo 1 and the minimum compressive strength of the concrete cores from Silo 4 tested as part of this evaluation. As designed, the silos satisfied the requirements of the current American Concrete Institute (ACI) requirements. However, because of the deterioration of the concrete, the silos no longer meet ACI requirements.

The following conclusions were derived from the current evaluation:

1) The silo domes do not appear to be in immediate danger of collapsing under dead and design live loads because the computed stresses are less than allowable.

   Under existing sustained loads, the wall membrane hoop stresses exceed the allowable stress but not the ultimate capacity. Thus, the existing safety margin is less than desired, but not enough to indicate near term structural failure.

2) Testing has shown that the material properties of the silo concrete have degraded such that a specific remaining life expectancy cannot be predicted. If no corrective actions are taken, the concrete may continue to degrade and the structure may ultimately fail.

3) The silo domes and/or walls will collapse under the assumed tornado loading. The maximum predicted stresses are hoop stresses that occur near the edge of the dome. Under the assumed tornado loads, both dome and wall hoop stresses exceed the ultimate as well as allowable stresses, and thus, no safety margin exists.

4) A comparison of allowable stresses and calculated dome stresses indicates that the protective cover placed on top of the central portion of each dome is not required. The cover creates local bending stresses which the

dome has not been designed to resist. However, even with the additional local stresses, the allowable limits under dead and live load are not exceeded. Also, the absence or presence of a dome cover does not significantly affect the critical hoop stresses near the edge of the dome during a tornado loading. Therefore, the protective cover need not be removed.

5) The combined embankment and content loads do not significantly affect the dome stresses.

6) Removal of the silo contents without removing the earthen embankments would result in extremely high compressive stresses in the wall, which would cause structural failure.

7) Removal of the earthen embankments without removal of the contents would result in higher than allowable tensile stresses. However, the wall is not expected to collapse due to this over stress because the posttensioning wires will be remobilized and provide additional strength. The dead load includes only a 100,000 psi stress contribution from the posttensioning wires. This represents a 30% loss from the design value of 140,000 psi.

8) The measured dome thickness (reported in the Camargo report) and concrete strengths are less than current ACI code requirements.

9) Cores obtained from Silo 4 contained reinforcing steel 1/8 in. and 3/8 in. in diameter. This is inconsistent with

information in the design drawings for the Silos.

3.2 Recommendations

The current study agrees with the Camargo report in that the condition of each of the silo domes must be considered structurally defective, with no definable life expectancy. It is recommended that one of the following alternatives should be undertaken:

1) Remove and dispose of the silo contents, and decontaminate and demolish the silos.

2) Construct an independent enclosure(s) around the silos to protect them from the effects of tornados and minimize the release of radon in case a silo dome should collapse because of further concrete degradation.

   If this alternative is selected, the enclosure(s) should be designed to provide a controlled environment for the ultimate removal of the silo contents.

3) Cover the residues inside the silo with a layer of free-flowing material that will minimize exposure of the contents and release of radon in case of failure of the silo domes.

   This alternative would add to the volume of contaminated waste and could make subsequent removal of the contents more difficult.

4) Construct a light, self-supporting structure around the domes that will provide a secondary barrier to minimize radon release if a dome should collapse because of further concrete degradation. Such a structure would differ from that in described above in that it would not be designed to prevent dome failure under tornado loading.

5) Take steps to minimize water coming in contact with the silo domes and walls. This includes placing additional waterproof coatings on the foam as required to help minimize further degradation of the concrete. In addition, perform periodic surveys to determine changes in the elevation of the top relative to the spring circle of each dome, and install instrumentation on top of the silos walls to detect changes in circumference. Such routine surveying and instrumentation will provide data with which to predict the behavior of the dome. This will provide an early warning of further concrete degradation that would mandate taking additional action.

Alternatives 2 through 5 are conceptual in nature, and studies will be required to evaluate their feasibility and cost. The alternatives range from proactive to reactive measures to minimize the potential for uncontrolled release of radon gas.

In addition, discrepancies in the diameter of reinforcing steel found in the core samples versus the drawing specifications should be resolved by further investigation.

4.0 DISCUSSION OF RISKS

A qualitative assessment of risks shows that the silos, in their current condition, will fail under tornado loading, and that continued degradation of the silo concrete will ultimately lead to dome collapse under dead load conditions. Either type of dome failure would result in an uncontrolled release of radon to the environment. The remaining life of each dome cannot be predicted accurately from available information. Computer analysis and concrete strength test results suggest that the domes could collapse at some time in the future. However, prestressed structures such as these silos have proven to be very durable, even in a deteriorated condition. Experience in demolishing such structures (Ref. 3-1) has shown that they have inherent strength that significantly exceeds their theoretical strength.

Further degradation of the silos must be minimized. Limiting infiltration of water precipitation into the porous concrete of the silos will decrease the inventory of water available in the concrete. This inventory of water in the concrete during freezing and thawing cycles could, through the years, completely destroy the structure. Water is also the medium through which alkali aggregate reaction occurs. However, preventing rainwater from coming in contact with the silo domes would not prevent the existing water in the silos or earthen embankments from migrating into the silo walls.

Based on the current analysis results and in recognition of the inherent strength of prestressed dome structures, the silo domes do not appear to be in immediate danger of collapse unless subjected to tornado loadings. However, the risk of failure does exist and should be reduced by implementing one of the recommendations listed in Section 3.2. Table 4-1 provides a qualitative comparison of the effectiveness of each suggested

Table 4-1
Comparative Risk of Uncontrolled Release of Radon

Alternative	Description	Risk Factor	Basis for Risk Factor
1	Remove contents and remediate silo	1	Dome failure before remedial action occurs
2	Construct tornado resistant structure	2	Same as Alternative 1 plus increased risk of damage to dome during construction of structure or structure not leak tight
3	Cover residues inside the silo with a free flowing cover material	4	Limited radon release resulting from perforation of covermaterial should the dome fail due to either tornado loading or further concrete degradation
4	Construct light	6	Extensive radon restructure as radon rlease due to failure barrier of both light structure and dome under tornado loading
5	Protect from rain and instrument concrete	8	Extensive radon release should the dome fail due to either tornado loading or further concrete degradation
6	No Action	9	Same as alternative 5 but with increased risk of dome failure due to further concrete degradation
	Dome failure with radon release	10	

alternative for reducing the risk of an uncontrolled release of radon gas. The risk factors listed in the table are based strictly on engineering judgement and not on theoretical analysis. The risk factors do not consider the probability of a tornado occurring at the site.

5.0 FIELD INVESTIGATIONS

In September 1989, during a two-day meeting to discuss the objectives of the study and evaluation described herein, BNI performed an informal visual examination of Silos 3 and 4. The BNI team was unable to inspect Silos 1 and 2 because the silos are backfilled and the domes are covered with foam and a self-supporting cap.

The concrete walls of Silo 3 showed considerable pattern cracking on the shot-crete coating. Efflorescence and steel oxidation were visible on the pattern-cracked areas. Silo 4 showed the same distress as Silo 3, with pattern cracking on the shot-crete walls and efflorescence of calcium carbonate or sodium silica gel. Inspection of the dome of Silo 4 revealed the same pattern cracking, as well as steel oxidation in numerous areas of the cracked posttensioned walls. Post-tensioning wires and concrete on Silos 3 and 4 showed excessive degradation and distress from weathering.

When the initial visual examination was completed, a work plan (Appendix D) was prepared to direct the sampling of Silo 4. The work plan delineated the prerequisite activities -- such as silo dewatering, air sampling, and safety measures and precautions -- to be performed prior to commencement of BNI's field activities. Core samples were taken of the silo dome, interior wall, and interior floor. A photographic record (Appendix E) of the coring activities was maintained. During the sampling activities the following observations were made.

1) The exterior walls of Silo 4 were covered in shot-crete with noticeable efflorescence causing a white buildup on the shot-crete exterior surface. The shot-crete on the wall was in fair condition except for the wall-dome interface area where deteriorated shot-crete was falling from the wall, exposing the posttensioning wire wrap. A sample of the shot-crete was removed from the walls for petrographic analysis.

2) The north half of the dome surface was spalling. Nine core holes were drilled into the dome (sample locations are shown on Figure 1 of Appendix D). Three cores were taken from the south half of the dome; six attempts were made to obtain a sample suitable for compressive strength testing from the north half of the dome. However, each attempt on the north half yielded concrete cores so fragmented that they were unsuitable for strength testing. The three dome samples from the south half (B91C02D, B9IC03, and B91C04D) were used for strength testing, and two of the fragmented samples were used for petrographic analysis.

3) During the process of obtaining core samples of the wall and floor in Silo 4, cracking and efflorescence were seen

throughout the interior dome and walls. Little evidence of concrete spalling was visible on the interior wall surface.

4) An asphaltic material had been applied around an apparent crack on the south side of the interior wall of Silo 4, indicating that interior repairs had been attempted at least once. The coated crack appears to have continued to propagate radially after the asphaltic material was applied, and indications of continued efflorescence after application of the asphaltic coating are also visible. Core samples taken from the northwest quadrant of the wall showed fractures as much as 2 in. long. Four wall samples were obtained for strength testing and one for petrographic analysis.

5) The condition of the floor could not be determined because it was covered with water and a layer of silty material. One floor sample was obtained for strength testing.

6.0 MATERIAL TESTING

6.1 Concrete Strength Testing

All concrete core samples obtained from the dome, walls and floor were cracked. Some samples were so fragmented that they were neither suitable for compressive nor tensile strength testing.

Three concrete core samples from the dome, four from the wall, and one from the floor were sent to the Geotek Engineering Company of Knoxville, Tennessee, for strength testing. The dome samples were tested for unconfined compressive strength in accordance with ASTM C39 (Ref. 6-1). The strength of the three dome cores ranged from 1306 to 2475 psi.

Three of the four samples obtained from the silo wall were tested for unconfined compressive strength in accordance with ASTM C39, and one was tested for splitting tensile strength in accordance with ASTM C496 (Ref. 6-2). The compressive strength of the cores from the silo wall ranged from 1463 to 2531 psi. The splitting tensile strength was 463 psi.

The one core sample obtained from the floor of the silo was tested for unconfined compressive strength in accordance with ASTM C39. Strength of that sample measured 3214 psi.

The detailed report of the strength testing performed by Geotek Engineering Company is provided in Appendix G.

6.2 Petrographic Analysis

Two dome samples, one wall sample, and one shot-crete sample were sent to Twin City Testing Corporation of St. Paul, Minnesota, for petrographic analysis and air-content determination in accordance with ASTM C856 (Ref. 6-3) and ASTM C457 (Ref. 6-4), respectively.

All concrete samples were fractured. The fractures were oriented both subhorizontal and subvertical to the long axis of the cores, and extended through the coarse aggregate. The concrete also appeared to have been placed with a medium to high slump and contained reactive rock particles of chert and silica (See Appendix G). Extensive carbonate deposits were seen along the fractures within the concrete samples. In addition, secondary deposits of alkali silica gel and calcium carbonate were found in cracks and voids with reaction rims around coarse aggregate particles indicating the aggregate was reactive.

The 2-inch shot-crete coating placed over the post tensioning wire wrap around the silo wall appeared to be relatively dense

with medium to low porosity. No evidence of microcracking or deleterious chemical reactions was observed in the shot-crete coating.

The detailed report of the petrographic analyses performed by Twin City Testing Corporation is provided in Appendix H.

6.3 Results of Material Testing

The Silo 4 wall and dome concrete had a compressive strength of 5050 psi at 28 days after the concrete was placed (Appendix C). The average dome compressive strength of 1948 psi after 37 years represents a loss of 61 percent of the strength of the dome. If the lowest compressive strength measured in the core (1306 psi) is used, it represents a 74 percent loss of strength in the concrete of the dome.

The cores of concrete from the wall had an average compressive strength of 2027 psi in the 1989 testing. This represents a 60 percent loss of strength. The lowest strength result (1463 psi) represents a loss of 71 percent of the wall's strength during the 37 year life of the silo.

The tensile strength core from the wall tested at a splitting tensile strength of 463 psi, which is excellent if it is an accurate result. Generally, tensile strength of concrete runs from 8 to 10 percent of its compressive strength. As one of the wall concrete core samples had a compressive strength of 1463 psi, a tensile strength range of 100 to 150 psi is a more realistic approximation.

Observations, test results indicating loss of strength, and past experience indicate that the quality of the concrete, after 37 years of exposure, is very poor. The laboratory analysis

indicates that the concrete was placed with medium to high slump. A high slump concrete, in general, is less dense, more porous, and less durable overall.

The reactivity, mentioned in the petrographic analysis report, generally occurs within 90 days after placement of concrete. It is responsible for the expansion of the concrete producing microcracking which allowed ingress of water to the concrete. Freeze-thaw conditions, through time, aggravated these conditions, increasing the size of the cracks and deterioration of the concrete.

The overall quality of the shot-crete sample was good. No evidence of microcracking or alkali-aggregate reaction was noted.

7.0 STRUCTURAL ANALYSIS

Finite-element analyses were performed 1) to verify the results of the previous studies (Model 1), 2) to determine the effect of the protective cover structure on the central portion of the dome (Model 2), and 3) to determine the present state of the structural integrity of the silo (Model 3). SAP90 Computer Program was used in the analysis (Ref. 7-1).

7.1 Finite-Element Models

Three-dimensional shell elements with bending and membrane actions were used to develop a finite-element model of a silo. Because a silo is approximately axisymmetrical, one quadrant of the silo was modelled, as shown in Figure 7-1, with proper symmetry conditions imposed along the radial boundaries. The primary disruption of the axisymmetry of the actual silo is the presence of the hatches and access holes on the dome. Three of these openings were included in the model. The previous studies indicated that the dome structure was the most critical in terms

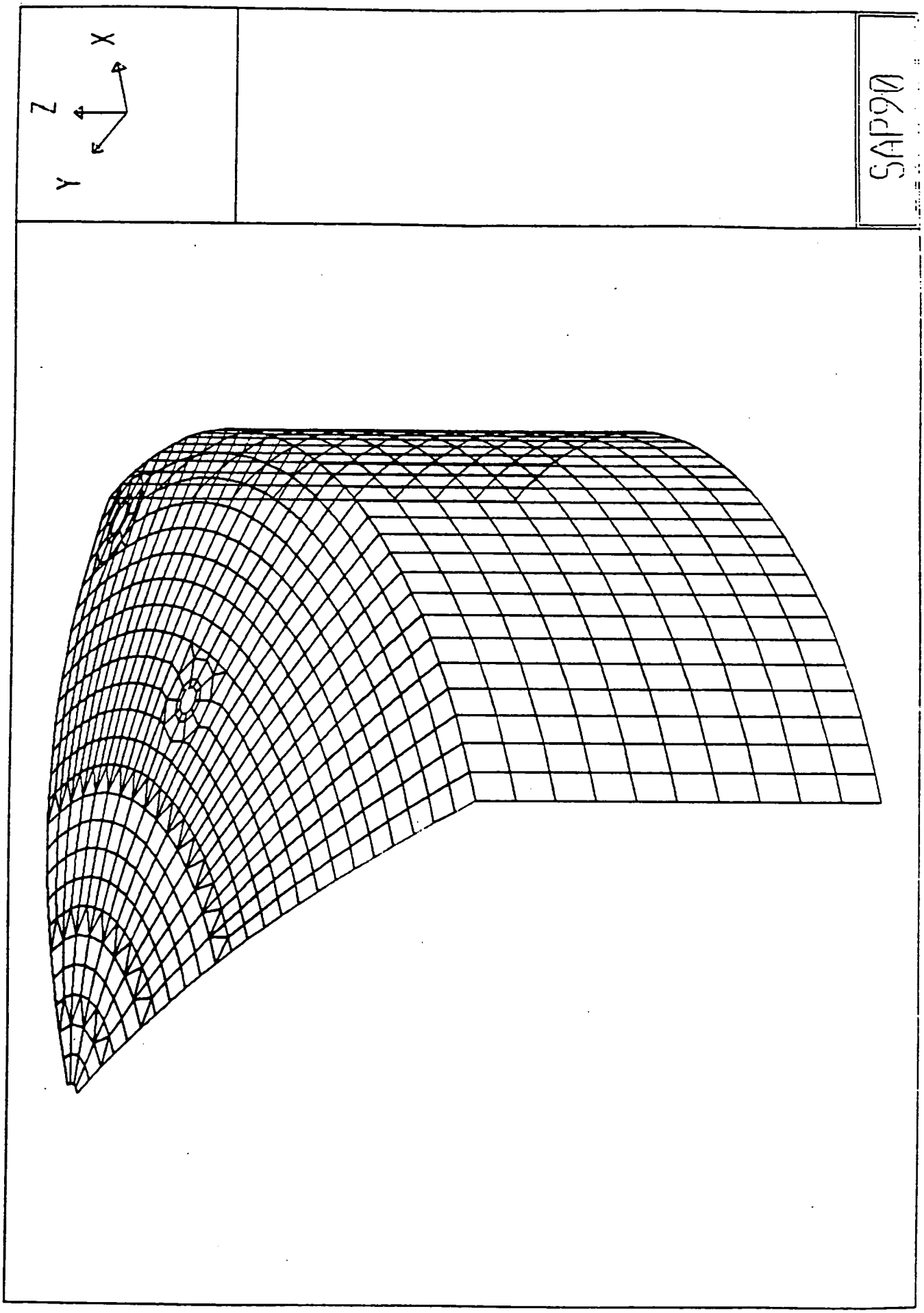

FIGURE 7-1: FINITE-ELEMENT MODEL OF SILO

of the structural integrity of an actual K-65 silo, and that the basemat was in reasonably good condition. Therefore, only the silo dome and wall were included in the present models.

The bottom of the wall was assumed to be pin-connected to the slab based on the previous studies. Thus, only translational degrees of freedom were restrained at the bottom edge of the model. Based on the detailed drawings, the joint between the dome and the wall was also assumed to be a pin-connection and was modeled such by using constraints. This is a diversion from the models used in the previous studies, where the wall-to-dome connection was assumed to be moment resisting. However, the net effect of using one model or the other can be observed only in a narrow band near the joint. As far as the general response of the dome and wall, there is no difference between the two models. The thicknesses of the elements represent averages of the measured values, ranging from 2.5 in. at the center of the dome to 7.25 in. near the edge. The elements near the openings range from 6 to 8 in. in thickness. The wall thickness is 7 to 8 in.

The reinforcing steel pattern and thicknesses provided in the design drawings for Silo 1 were utilized in the model of the silo.

The above description is common to all three models. The differences between the models are as follows:

- Model 1 does not have the protective cover at the central portion of the dome. Models 2 and 3 have the same model geometry as Model 1, but the weight of the protective cover, the live load, and the tornado loads, which would act on the protective cover, were

applied as resultant line loads on the dome along the circumference of the protective cover.

- The material properties used in Models 1 and 2 are those measured and used in the previous studies by Camargo. Model 3 uses the concrete strengths measured as part of the present study. For the elastic stress analysis, only the modulus of elasticity and Poisson's ratio for the material are used in defining the model.

7.2 Loads and Load Combinations

The finite-element models were analyzed for the following loads:

- Dead load (DL) - includes the weight of the structure and the axial and circumferential post-tensioning load on the wall.

- Live load (LL) - 20 psf snow load on the dome.

- Embankment pressure (E) - a triangular soil pressure on the exterior face of the wall based on a soil density of 130 pcf and a K (lateral earth pressure coefficient) factor of 0.5.

- Contents pressure (C) - a triangular pressure distribution on the interior face of the wall based

on a contents density of 100 pcf and a K factor of 1.0.

- Tornado pressure (TP) - 401 psf pressure on the outside of the dome.[2]

- Tornado suction (TS) - 432 psf suction on the outside of the dome.[2]

The stress results obtained under each load case were combined according to Table 7-1, where X indicates the loads included in each combination. Silo model data and analysis results are tabulated in Appendix I.

7.3 Discussion of Results

The stresses computed for each load combination and each model are given in Appendix I. A summary of these stresses is listed in Tables 7-2 through 7-9. (All figures and tables discussed hereafter can be found following this section of the report). Figures 7-2 through 7-5 show the deflected shape of the model under dead load, live load, contents load, and the embankment load, respectively, to depict the general behavior of the silo under each type of load. Figures 7-6 and 7-7 are sample hoop membrane force contours.

7.3.1 Comparison With Previous Results

Table 7-2 shows a comparison of stresses in the dome under dead load calculated in the previous studies and in the present study. Analytically computed stresses at the center of the dome are also

---

[2]The tornado suction and pressure forces used in this study are the same values used in the Camargo report. These forces correspond to the design basis tornado for Region I (east of the Rocky Mountains) as defined in U. S. NRC Regulatory Guide 1.76.

included in Table 7-2 for comparison. The Camargo results were computed using a model with triangular axisymmetric solid elements. Bechtel results are computed from quadrilateral shell elements. The computer output of the Camargo analysis, which was reviewed to extract the data in Table 7-2, shows an irregular variation of the stresses between adjacent elements. This irregularity is particularly evident in the central portion of the dome model. This is a typical problem with certain kinds of triangular finite elements originating from the theoretical formulation of the algorithm. In spite of this, there is a general agreement between the three sets of results in Table 7-2. The discrepancies are not large enough to invalidate the conclusions of either study.

Table 7-3 shows the stress results summary for Model 1. In the Camargo studies, 41 psi tension and 190 psi compression were reported near the center and edge of the dome, respectively, under load combination 5. The present study confirms the compressive stress (214 psi) near the edge of the dome, but does not indicate any tensile stresses in the dome under load combination 5. A review of the computer output of the Camargo study showed that the 41 psi tensile stress reported was in a small region and included some bending stress contribution. Nearby elements do not indicate the presence of any tension. Thus, this tensile stress should be attributed to the behavior of triangular finite elements and should not be considered a real stress.

7.3.2 Model 1 Results

Except for load combinations 7 and 8, all the membrane stresses are compressive in the dome of the silo, as shown in Table 7-3. For load combination 7, the hoop stress near the edge of the dome becomes tensile. This is the load combination with the tornado pressure on the dome. As the dome is pushed down by the tornado

pressure, the edge of the dome is pushed outward. This creates the tensile force in the hoop direction along the edge of the dome. The same behavior is exhibited under live and dead loads, but without the extreme tornado pressure, the compressive stresses due to posttensioning are not overcome to show a net tensile stress. Load combination 8, which includes the tornado suction, results in stresses that have opposite sign to the load combination 7 stresses as expected.

7.3.3 Model 2 Results

Model 2 stress results are summarized in Table 7-4. The stresses in the central portion of the dome are less than those in Model 1 (Table 7-3). The edge stresses are less affected than the dome center stresses by the addition of the protective cover. In Model 2 the stresses in the dome at 15-ft radius, however, are significantly higher in the hoop direction than those in Model 1. An important effect of the cover structure on the integrity of the dome is the meridional moment it causes in the dome along the circumference where the cover is supported. The dome does not have any moment reinforcement to resist this loading. Under dead and live loads the nominal bending stresses are 90-95 psi in this part of the dome, assuming a linear stress distribution. For load combinations 7 and 8 (tornado pressure and suction), this bending stress is as large as 1300 psi.

7.3.4 Model 3 Results

The stresses shown in Table 7-5 for Model 3 are very similar to the stresses obtained using Model 2. This is expected because the difference between the two models is only in the modulus of elasticity used for concrete. The variation of this parameter within a model is more important than its magnitude in affecting the computed stresses. A smaller modulus of elasticity was used in Model 3 due to significantly reduced concrete strengths

identified from testing. However, the variation of this parameter from one model to another is not significant. Therefore, stress results are only slightly affected because of this modification in the model.

In addition to the dome where this analysis has been focused, the stresses in the wall also were computed. Maximum wall stresses are shown in Table 7-6, which indicates that the wall does not go into membrane tension under any of the load combinations. Maximum stresses are produced by the tornado loading.

7.3.5 Comparison of Computed and Allowable Stresses

The stresses computed using Model 3 are compared to the allowable stresses in Table 7-7. Model 3 results are used here because this model represents the current state of the silo.

a) Allowable Stresses

Since the loads were combined without applying any load factors, the allowable stress approach was used to evaluate the silo. The allowable stresses were computed based on the reinforcement shown in the drawings and the minimum compressive strength of the concrete cores that were tested as part of the present study.[3] The measured concrete strengths are much less than the design strength, which accounts for a significant deterioration of the concrete. Concrete strengths of 1,306 psi for the dome and 1,463 psi for the wall were used in the evaluation. The minimum values

---

[3] **The designed reinforcement of the general area of the dome is a wire mesh of W4 X W4 at 4 in. X 4 in. The bar diameter of this wire mesh is 0.226 in. Some of the concrete samples taken from the dome in Silo 4 contain 0.125 in. diameter bars. The drawings do not show any 0.125 in. diameter bars in the dome. This discrepancy should be resolved by further investigation.**

are conservative and were chosen because the deterioration of the concrete could continue further. Because of the deterioration of the concrete, the silo in its present condition does not meet current ACI concrete strength and shell thickness requirements for the design of storage silos (Refs. 7-2, 7-3).

Allowable buckling load of the dome was computed using the formula recommended by ACI for the calculation of minimum shell thickness with a safety factor of 4. This approach is the same as the one used in the Camargo study. However, in that study a safety factor of 4 was applied on the critical load obtained from the ACI formula, which already contained the safety factor. The concrete strength used in the current study for allowable buckling load calculation is about 65 percent of that used in the Camargo study. Hence, considering the differences in safety factors and material strength, the buckling allowables used in the present study are approximately 3 times higher than the allowable used in the previous study. The allowable buckling load was converted to nominal stresses in various parts of the dome for comparison with computed stresses in Tables 7-7 and 7-8.

The allowable tensile force is the reinforcement area multiplied by the ACI allowable stress of 24,000 psi for wire mesh reinforcement in shells. This force is divided by the shell thickness to obtain the nominal allowable tensile stresses shown in Table 7-7.

Stresses in the silo wall are summarized in Table 7-9 for selected load combinations including the lateral load. The table shows that certain stresses exceed the allowable limits. The highest overstress in Table 7-9 is for the hoop membrane compression under load combination 4 which includes the embankment pressure without contents.

Load combination 5, where the contents are added to load combination 4, shows that the above overstress is reduced by a factor of three but still exceeds the allowable stress.

In the case of load combination 9, which includes dead load (including posttensioning) and pressure due to contents, compressive stresses are within allowable limits but membrane tensile stresses in the hoop direction exceed the allowable.

b) Discussion

Maximum stresses in the dome and wall are compared with the allowable stresses in Table 7-7. The greatest difference between allowable stress and computed stresses is the hoop stress at the dome edge. The computed stresses are not affected by the presence or absence of the dome cover.

At the central part of the dome the computed stresses are less than the allowable stresses, indicating that the protective cover serves its purpose in this part of the shell. However, it must be noted that the protective cover itself was not analyzed in this study. It is very likely that the cover will collapse under a tornado load and expose the protected portion of the dome to the tornado loading. Regardless of the condition of the protective cover, under a tornado loading the dome stresses would be several times larger than the allowables as shown in Table 7-7.

Table 7-8 is a summary of the present state of stress in the silo dome under dead plus live loads as compared to the allowables. All computed stresses are less than allowable, with the computed hoop stress at the dome edge being closest to the allowable stress.

Table 7-1
LOAD COMBINATIONS

Load Combination	Loads Included	Model 1	Model 2	Model 3
1	DL	X	X	X
2	DL+LL	X	X	X
3	--- NOT USED ---			
4	DL+LL+E	X	X	X
5	DL+LL+C+E	X	X	X
6	--- NOT USED ---			
7	DL+TP+C+E	X	X	X
8	DL+TS+C+E	X	X	X
9	DL+C	X	X	X
10	--- NOT USED ---			

Legend
DL = dead load
LL = live load (snow load)
C = contents load
E = earthen embankment load
TP = tornado pressure load, and
TS = tornado suction load.

Table 7-2
COMPARISON OF SELECTED STRESSES
OBTAINED IN PREVIOUS AND PRESENT STUDIES

Loading	Stress Type	Stress Location	Stress (psi) Camargo	Bechtel	Analytical*
Dead load including posttension	Hoop membrane	Near center of dome	-92	-50	-44
		Near edge of dome	-180	-279	N/C(**)
	Hoop bending	Near center of dome	±26	±1	0
		Near edge of dome	±10	±41	N/C
	Meridional membrane	Near center of dome	-80	-41	-44
		Near edge of dome	-45	-35	N/C
	Meridional bending	Near center of dome	0	±2	0
		Near edge	±32	±40	N/C

(*) Source: Ugural, A. C. Stress in Plates and Shells, New York: McGraw-Hill, 1981.

(**) N/C = not computed.

Table 7-3
MEMBRANE STRESSES IN THE DOME OBTAINED USING MODEL 1

Load Combination*	Location	Hoop Stress (psi) Tension	Hoop Stress (psi) Compression	Meridional Stress (psi) Tension	Meridional Stress (psi) Compression
1	Center	0	-50	0	-41
	15-ft radius	0	-48	0	-42
	Edge	0	-270	0	-35
2	Center	0	-80	0	-67
	15-ft radius	0	-70	0	-65
	Edge	0	-208	0	-43
4	Center	0	-80	0	-67
	15-ft radius	0	-70	0	-65
	Edge	0	-206	0	-43
5	Center	0	-80	0	-67
	15-ft radius	0	-70	0	-65
	Edge	0	-214	0	-43
7	Center	0	-652	0	-560
	15-ft radius	0	-502	0	-512
	Edge	970	0	0	-180
8	Center	599	0	519	0
	15-ft radius	442	0	465	0
	Edge	0	-1620	119	0
9	Center	0	-50	0	-41
	15-ft radius	0	-48	0	-42
	Edge	0	-278	0	-36

* See Table 7-1.

Table 7-4
MEMBRANE STRESSES IN THE DOME OBTAINED USING MODEL 2

Load Combination*	Location	Hoop Stress (psi) Tension	Hoop Stress (psi) Compression	Meridional Stress (psi) Tension	Meridional Stress (psi) Compression
1	Center	0	-48	0	-39
	15-ft radius	0	-71	0	-48
	Edge	0	-263	0	-36
2	Center	0	-43	0	-35
	15-ft radius	0	-131	0	-61
	Edge	0	-199	0	-44
4	Center	0	-43	0	-35
	15-ft radius	0	-131	0	-61
	Edge	0	-198	0	-43
5	Center	0	-43	0	-35
	15-ft radius	0	-131	0	-61
	Edge	0	-206	0	-44
7	Center	52	0	42	0
	15-ft radius	0	-1259	0	-313
	Edge	1015	0	0	-184
8	Center	0	-155	0	-126
	15-ft radius	1208	0	238	0
	Edge	0	-1653	123	0
9	Center	0	-48	0	-39
	15-ft radius	0	-71	0	-48
	Edge	0	-271	0	-36

* See Table 7-1.

Table 7-5
MEMBRANE STRESSES IN THE DOME OBTAINED USING MODEL 3

Load Combination*	Location	Hoop Stress (psi) Tension	Hoop Stress (psi) Compression	Meridional Stress (psi) Tension	Meridional Stress (psi) Compression
1	Center	0	-48	0	-39
	15-ft radius	0	-71	0	-48
	Edge	0	-265	0	-36
2	Center	0	-43	0	-35
	15-ft radius	0	-131	0	-61
	Edge	0	-201	0	-44
4	Center	0	-43	0	-35
	15-ft radius	0	-131	0	-61
	Edge	0	-203	0	-44
5	Center	0	-43	0	-35
	15-ft radius	0	-131	0	-61
	Edge	0	-207	0	-44
7	Center	53	0	43	0
	15-ft radius	0	-1259	0	-313
	Edge	1006	0	0	-184
8	Center	0	-157	0	-128
	15-ft radius	1208	0	238	0
	Edge	0	-1645	123	0
9	Center	0	-48	0	-39
	15-ft radius	0	-71	0	-48
	Edge	0	-269	0	-36

* See Table 7-1.

Table 7-6
STRESSES IN THE SILO WALL USING MODEL 3

Stress Type	Stress (psi)	Load Combination*	Location
Hoop Membrane			
Tension	-	-	-
Compression	-1498	8	Top
Hoop bending	±212	8	Top
Meridional membrane			
Tension	-	-	-
Compression	-351	7	Bottom
Meridional bending	±1025	8	Top

* See Table 7-1

Table 7-7
MODEL 3 MAXIMUM STRESSES AND ALLOWABLES

Stress Type	Stress (psi) Allowable	Stress (psi) Computed	Load Combination*	Location
Hoop tension	96	53	7	Dome center
Hoop compression	-198	-157	8	Dome center
Meridional tension	96	43	7	Dome center
Meridional compression	-198	-39	1	Dome center
Hoop tension	80	1208	8	Dome at 15-ft radius
Hoop compression	-235	-1259	7	Dome at 15-ft radius
Meridional tension	80	238	8	Dome at 15-ft radius
Meridional compression	-310	-313	7	Dome at 15-ft radius
Hoop tension	34	1006	7	Dome edge
Hoop compression	-235	-1645	8	Dome edge
Meridional tension	34	123	8	Dome edge
Meridional compression	-588	-184	7	Dome edge
Hoop compression	-263	-1498	8	Wall
Meridional compression	-658	-351	7	Wall

* See Table 7-1.

1. Hoop tension allowables are based on 4 in. x 4 in. W4 x W4 wire mesh reinforcement with 24 ksi of allowable stress.

2. Allowable compressive stresses are based on the lower of the buckling capacity and 18 and 45 percent of the concrete strength for hoop and meridional directions, respectively.

3. Local stresses near the hatches on the dome are not included in this table.

Table 7-8
DOME COMPRESSIVE STRESSES UNDER DEAD PLUS LIVE LOADS AND ALLOWABLES USING MODEL 3

Stress Type	Stress (psi) Allowable	Stress (psi) Computed	Location
Hoop	-198	-43	Dome center
Meridional	-198	-35	Dome center
Hoop	-235	-131	Dome at 15-ft radius
Meridional	-310	-61	Dome at 15-ft radius
Hoop	-235	-201	Dome edge
Meridional	-588	-44	Dome edge

Table 7-9
STRESSES IN THE SILO WALL FOR SELECTED LOAD COMBINATIONS

Load Combination*	Stress Type	Stress (psi)
4	Hoop membrane tension	0
	Hoop membrane compression	-1245(**)
	Hoop bending	160
	Meridional membrane tension	0
	Meridional membrane compression	-264
	Meridional bending	802(**)
5	Hoop membrane tension	0
	Hoop membrane compression	-396(**)
	Hoop bending	47
	Meridional membrane tension	0
	Meridional membrane compression	-258
	Meridional bending	236
9	Hoop membrane tension	174(**)
	Hoop membrane compression	-248
	Hoop bending	28
	Meridional membrane tension	0
	Meridional membrane compression	-249
	Meridional bending	141

* See Table 7-1.
(**) These stresses exceed the allowables given below:

Hoop compression	:	263 psi
Hoop tension	:	44 psi
Meridional membrane compression	:	658 psi

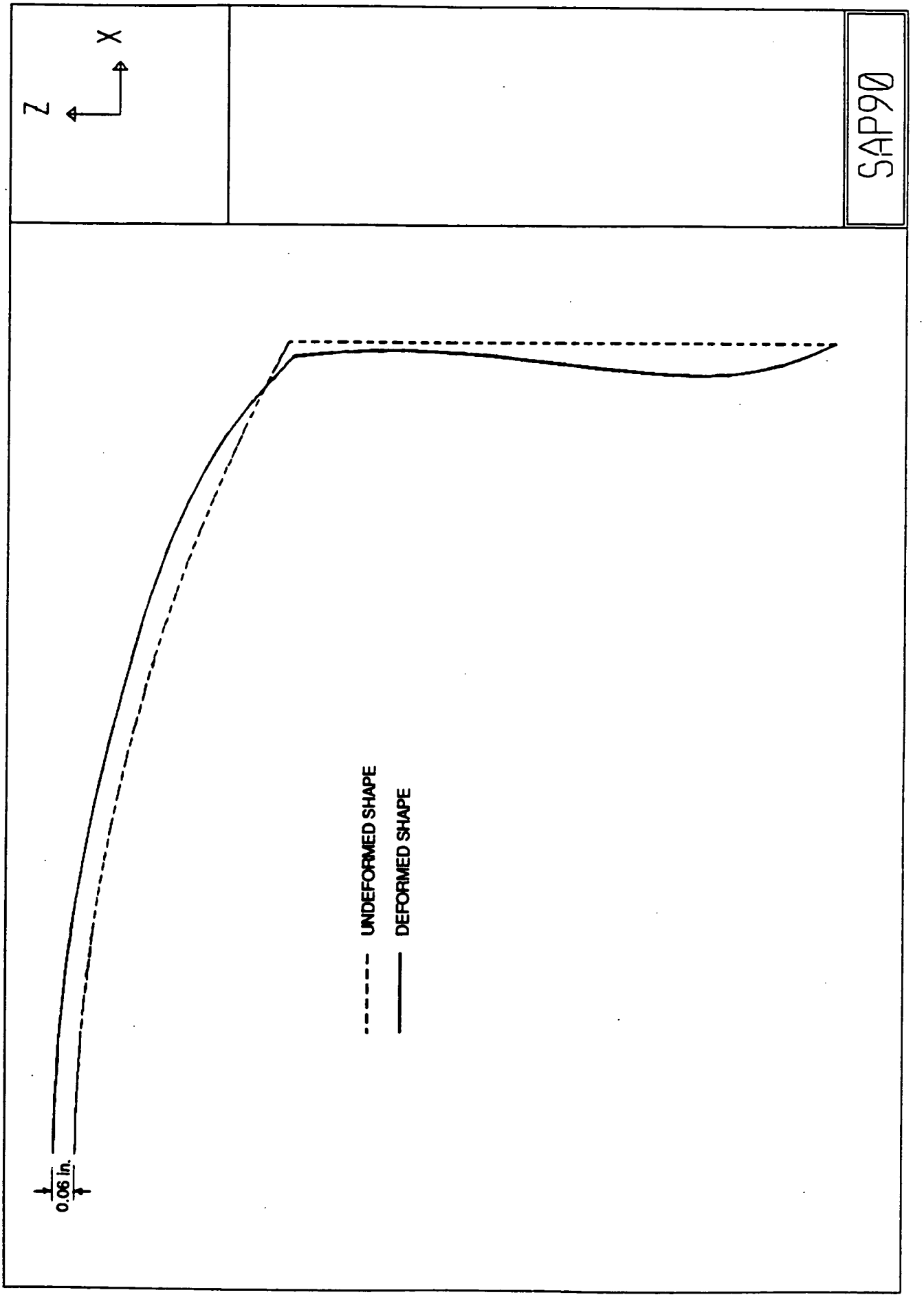

FIGURE 7-2: DEFORMED SHAPE - DEAD LOAD

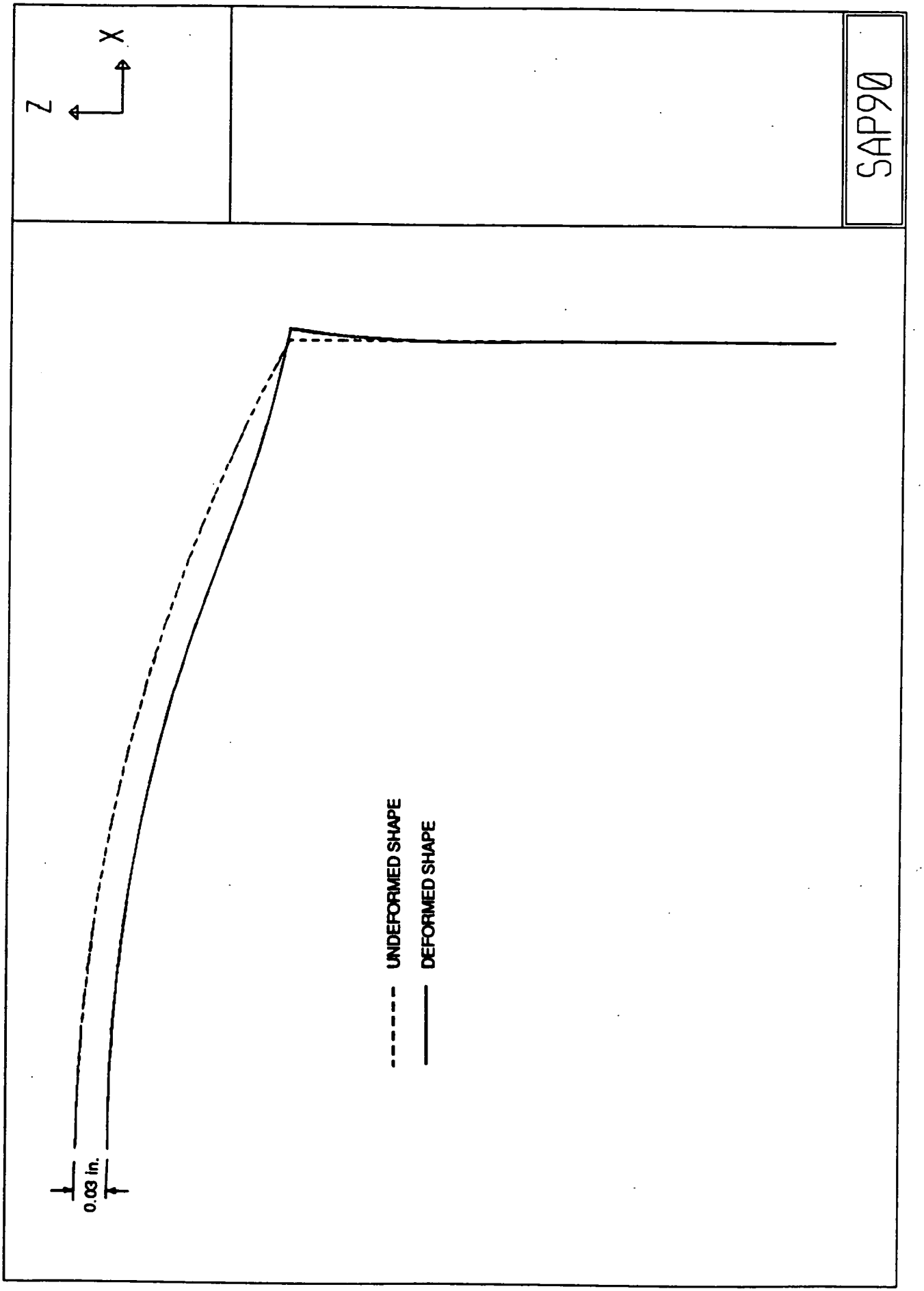

FIGURE 7-3: DEFORMED SHAPE - LIVE LOAD

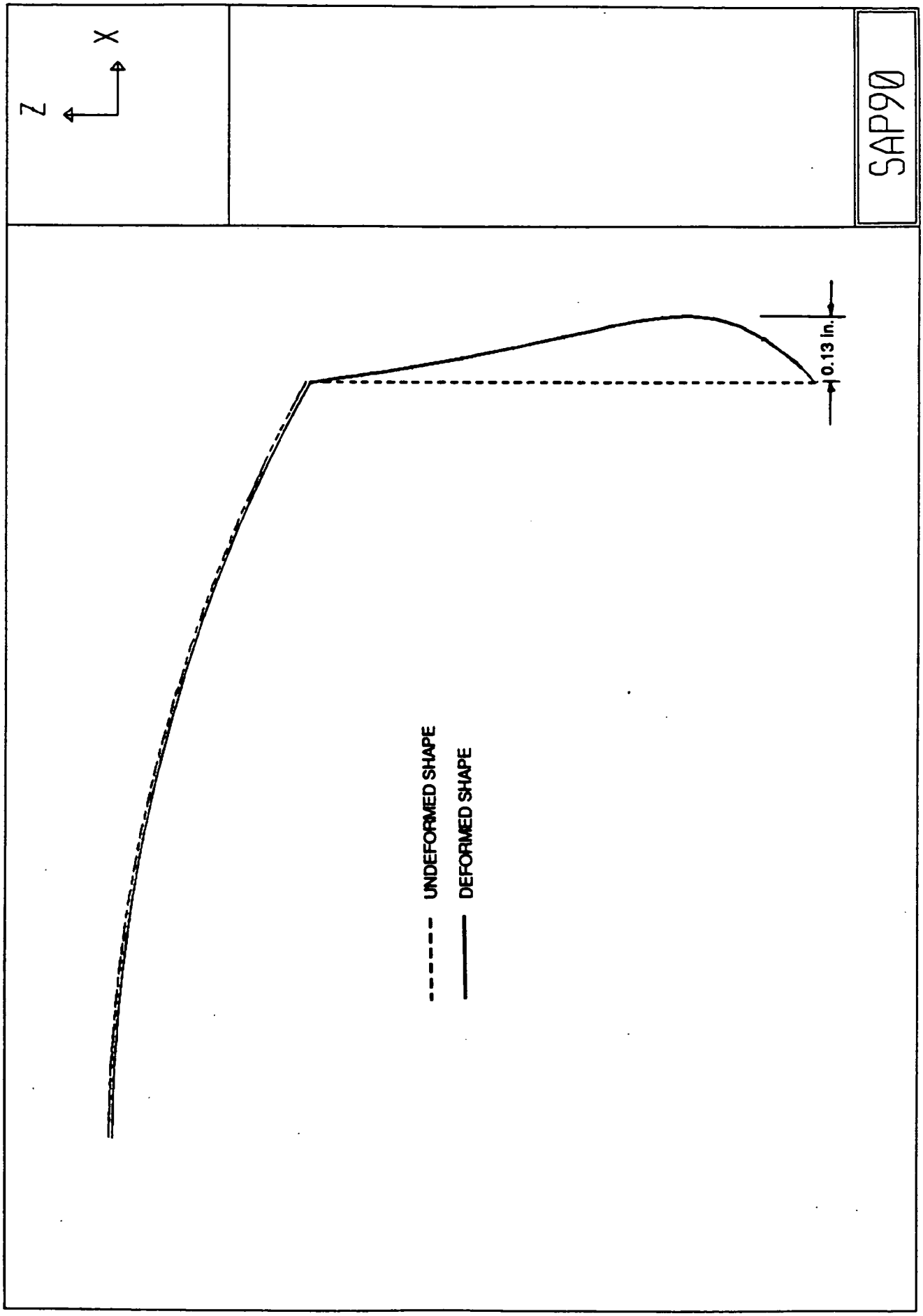

FIGURE 7-4: DEFORMED SHAPE - CONTENTS PRESSURE

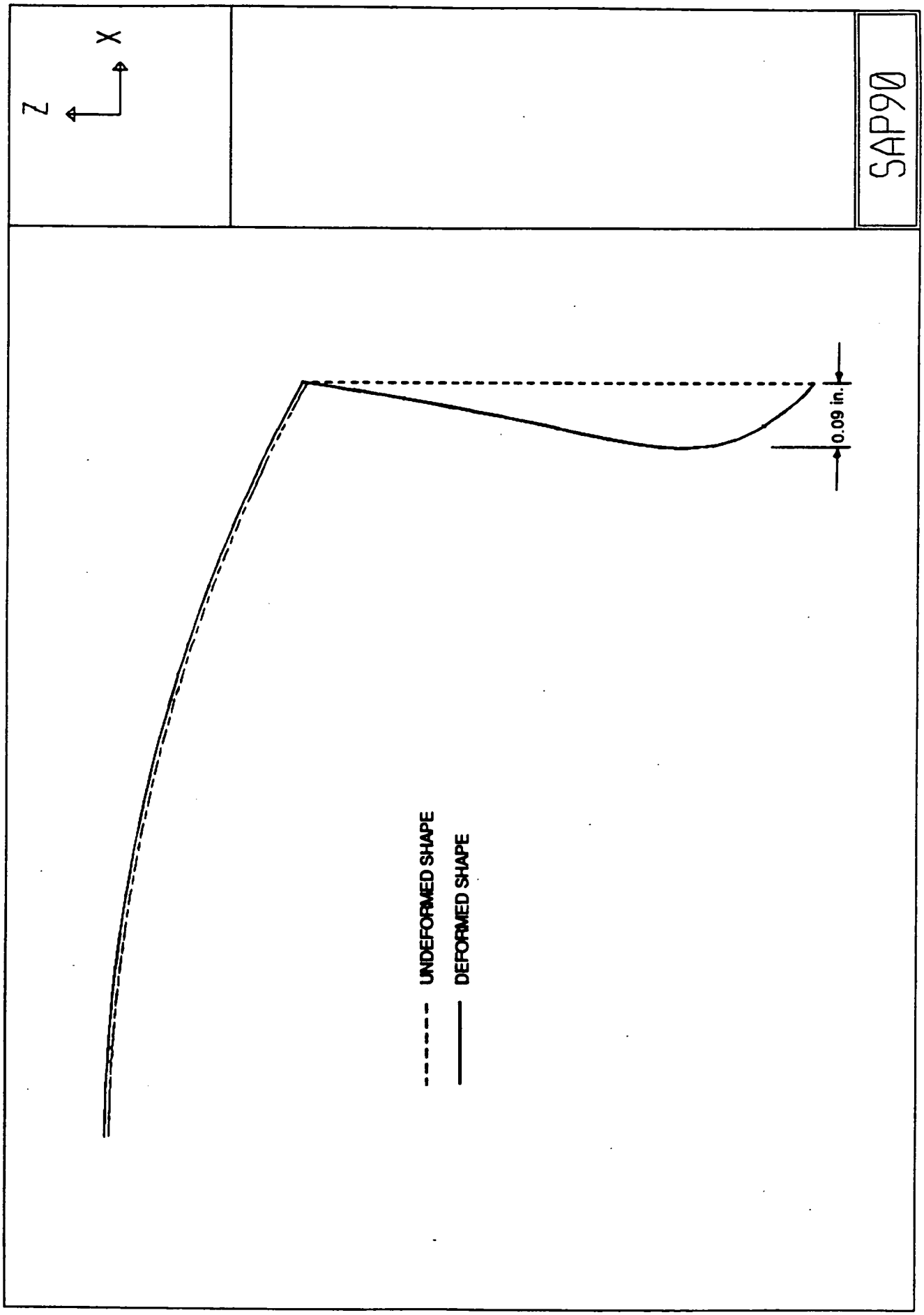

FIGURE 7-5: DEFORMED SHAPE - EMBANKMENT PRESSURE

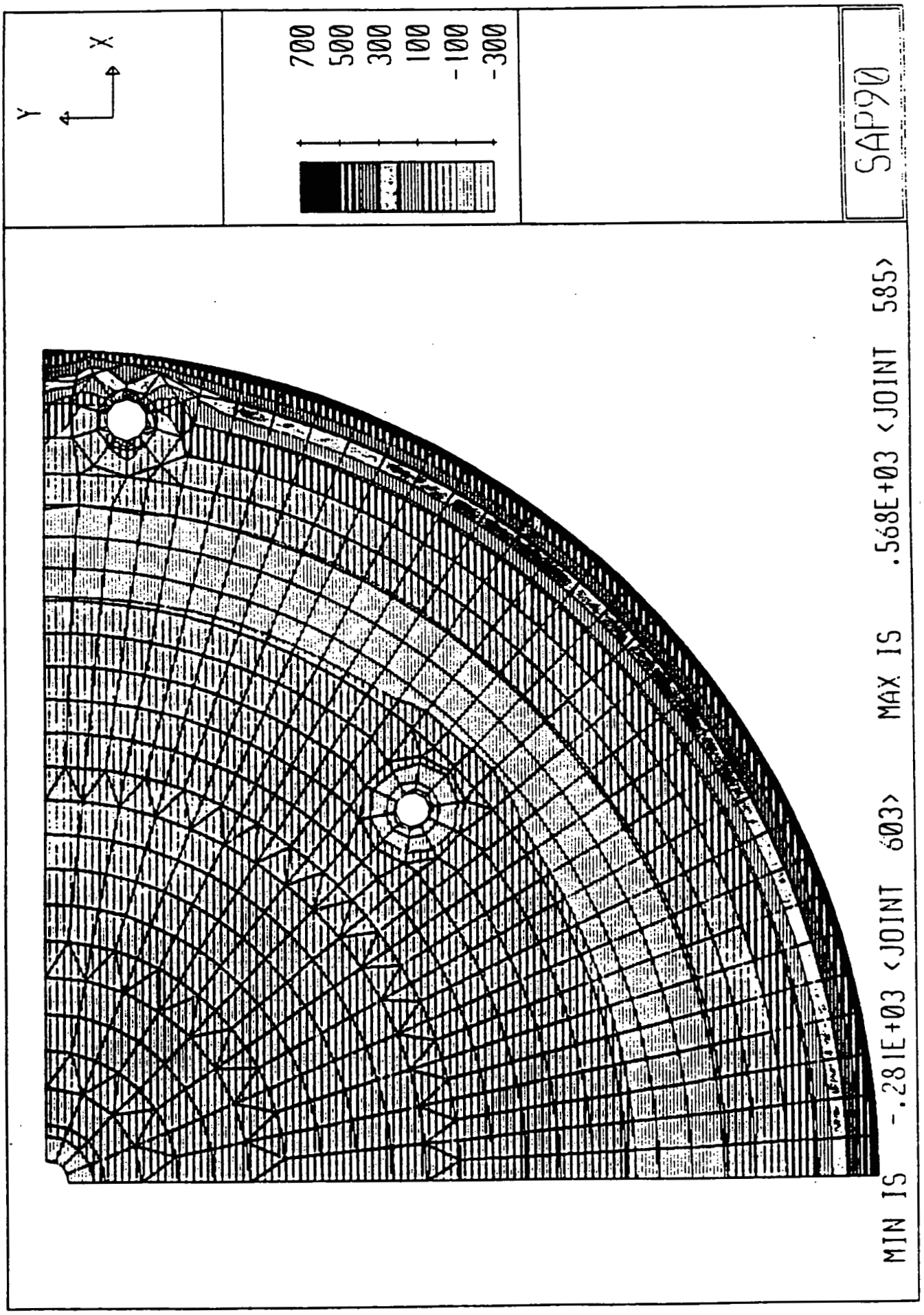

FIGURE 7-6: HOOP FORCES IN DOME - LIVE LOAD ONLY

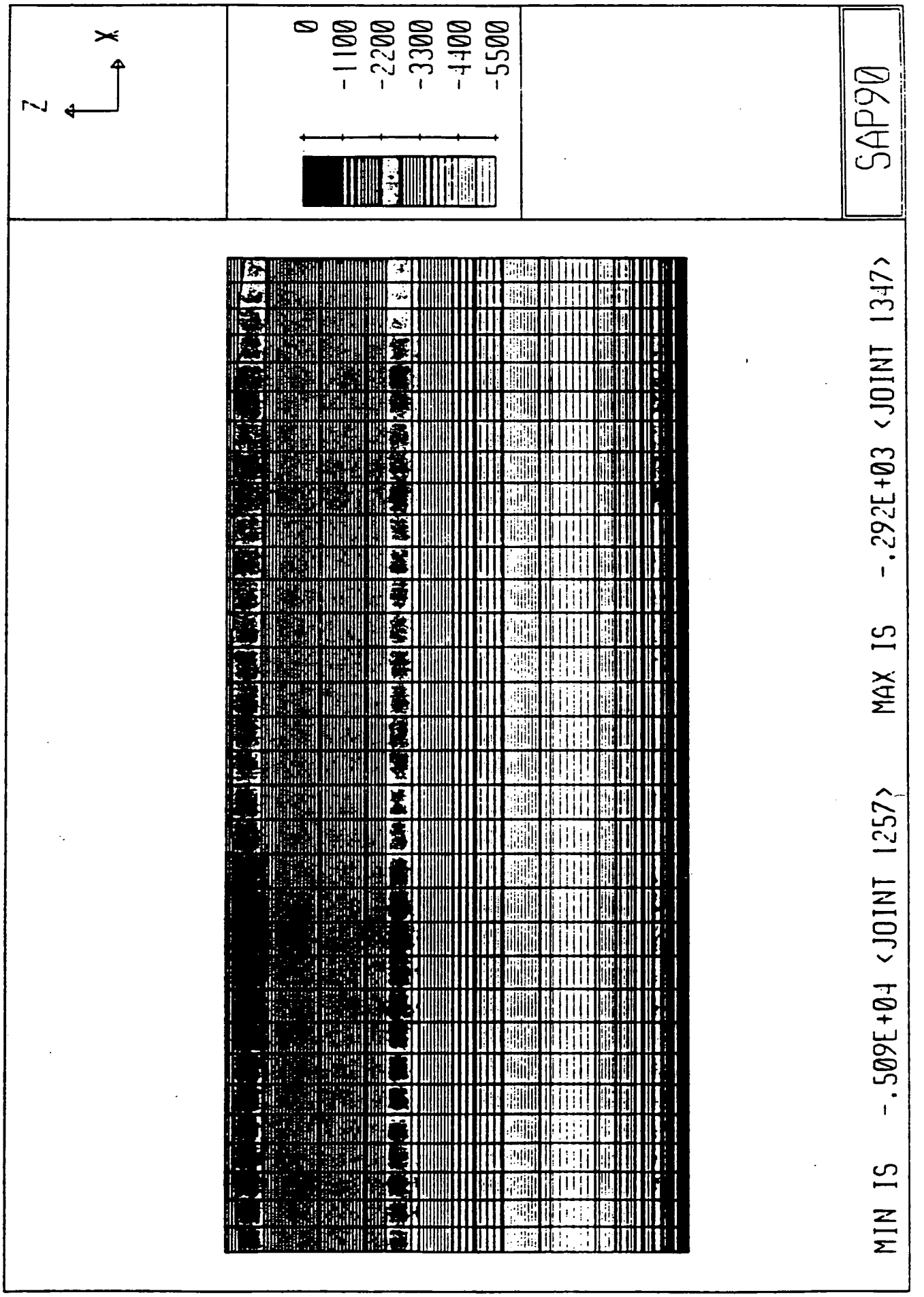

FIGURE 7-7: HOOP FORCES IN WALL - DEAD LOAD ONLY

8.0 REFERENCES

1-1 Camargo Associates, Limited. K-65 Silos Study & Evaluation Report, Cincinnati, OH, February 1986.

1-2 Camargo Associates, Limited. Metal Oxide and Empty Silo Study & Evaluation Report, Cincinnati, OH, May 1986.

3-1 Morris Schupack and Randell W. Poston, "Durability of Prestressed Concrete Silos," Concrete International, October 1989, pp. 51 - 58.

6-1 ASTM C39 Test Method for Compressive Strength of Cylindrical Concrete Specimens.

6-2 ASTM C496 Test Method for Splitting Tensile Strength of Cylindrical Concrete Specimens.

6-3 ASTM C856 Practice for Petrographic Examination of Hardened Concrete.

6-4 ASTM C457 Recommended Practice for Microscopical Determination of Air-Void Content and Parameters of the Air-Void System in Hardened Concrete.

7-1 SAP90, A Series of Computer Programs for the Static and Dynamic Finite Element Analysis of Structure, Edward L. Wilson and Ashraf Habibullah, Computers & Structures, Inc., Berkeley California, 1988.

7-2 Design and Construction of Circular Wire and Strand Wrapped Prestressed Concrete Structures, Reported by ACI Committee 344, American Concrete Institute, Detroit, Michigan, 1988.

7-3 Design and Construction of Circular Prestressed Concrete Structures with Circumferential Tendons, Reported by ACI Committee 34, American Concrete Institute, Detroit, Michigan, 1988.

7-4 Concrete Shell Buckling, Edited by Egor P. Popov and Stefan J. Medwadowski, Publication SP-67, American Concrete Institute, Detroit, Michigan, 1981.